OFF MASS SHELL EFFECTS IN ASSOCIATED PRODUCTION OF THE TOP QUARK PAIR AND HIGGS BOSON AT A LINEAR COLLIDER*

Karol Kołodziej[†], Szymon Szczypiński[‡]

Institute of Physics, University of Silesia
Uniwersytecka 4, 40-007 Katowice, Poland

We discuss effects related to the fact that the final state particles of the reaction $e^+e^- \to t\bar{t}H$ are actually produced and they decay off mass shell. For the intermediate mass Higgs boson, which decays preferably into a $b\bar{b}$-quark pair, the reaction will be observed through reactions with 8 fermions in the final state. Such reactions, already in the lowest order of the standard model, receive contributions typically from a few dozen thousands of the Feynman diagrams, the vast majority of which constitute background to the signal of associated production of the top quark pair and Higgs boson. In order to illustrate pure off mass shell effects we neglect the background contributions and compare the "signal" cross section with the cross section in the narrow width approximation for $e^+e^- \to bu\bar{d}\,\bar{b}\mu^-\bar{\nu}_\mu\,b\bar{b}$, which is one of possible detection channels of the associated production of the top quark pair and Higgs boson at a linear collider.

PACS numbers: 14.65.Ha, 14.80.Bn

1. Introduction

If the Higgs boson exists in Nature then it will be most probably discovered at the Large Hadron Collider, but the accurate study of its production and decay properties, which is crucial for verification of electroweak (EW) symmetry breaking mechanism, can be best performed in a clean environment of e^+e^- collisions at the future International Linear Collider (ILC) [1]. The study would be of the utmost importance for establishment of the Standard Model (SM) or possibly some of its extensions as, *e.g.* the

[†] `kolodzie@us.edu.pl`
[‡] `simon@server.phys.us.edu.pl`

minimal supersymmetric SM (MSSM) or some of more general supersymmetric models as the theory of the EW interactions. The Higgs boson mass m_H can be constrained in the framework of SM by the virtual effects it has on precision EW observables. The combined value of the top quark mass measured at Tevatron and the combined W-boson mass [2] give a central value of $m_H = 85^{+39}_{-28}$ GeV and an upper limit of 166 GeV, both at 95% CL, in agreement with combined results on the direct searches for the Higgs boson at LEP that lead to a lower limit of 114.4 GeV at 95% CL [3]. These constraints indicate that the SM Higgs boson should be searched for in the mass range just above the lower direct search limit [4].

If the Higgs boson mass is below the top quark pair threshold, $m_H < 2m_t$, then the Higgs Yukawa coupling to the top quark g_{ttH} can be directly determined in the process of associated production of the top quark pair and Higgs boson [5]

$$e^+e^- \to t\bar{t}H \,. \tag{1}$$

The lowest order SM Feynman diagrams of reaction (1), with the neglect of the scalar boson couplings to electrons, are shown in Fig. 1. As the
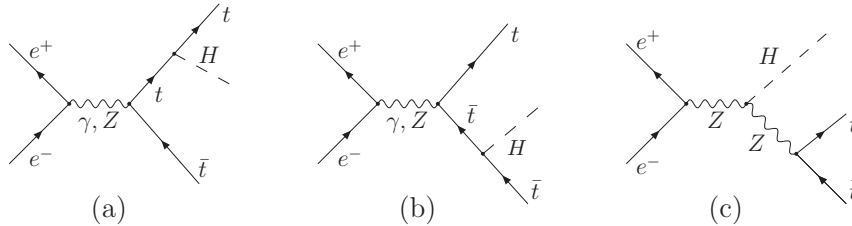

Fig. 1. Feynman diagrams of reaction (1) to the lowest order of SM with the neglect of the scalar boson couplings to electrons.

contribution of the Higgs boson emission off the virtual Z-boson line, which is represented by the diagram in Fig. 1(c), is small with respect to the Higgsstrahlung off the top quark line illustrated in Fig. 1(a) and 1(b), the SM lowest order cross section of reaction (1) becomes practically proportional to g_{ttH}^2. This fact makes reaction (1) so sensitive to the Higgs Yukawa coupling to the top quark. Because of its numerical value close to 1, precise determination of g_{ttH} may play an indispensable role in our understanding of the whole mass generation mechanism of SM.

Because of their large decay widths, the t- and $\bar{t}$-quark of reaction (1) almost immediately decay into bW^+ and $\bar{b}W^-$, respectively, the W-bosons subsequently decay into 2 fermions each and the Higgs boson, if it is lighter

than 140 GeV, decays dominantly into a $b\bar{b}$-quark pair. Thus reaction (1) will be actually detected at the ILC as a reaction of the form

$$e^+e^- \rightarrow bf_1\bar{f}'_1\bar{b}f_2\bar{f}'_2b\bar{b}, \tag{2}$$

where $f_1, f'_2 = \nu_e, \nu_\mu, \nu_\tau, u, c$ and $f'_1, f_2 = e^-, \mu^-, \tau^-, d, s$. The three possible detection channels of (2), which correspond to the decay modes of the W-bosons resulting from decays of the t- and $\bar{t}$-quark in the 'signal" diagrams of reaction (1), are

1. hadronic channel: eight jets (38 %),

2. semileptonic channel: lepton and six jets (37 %),

3. leptonic channel: two leptons and four jets (25 %).

In addition to the analysis in Ref. [5], reaction (1) has been extensively studied in literature. The QCD radiative corrections to (1) were calculated in [6], $\mathcal{O}(\alpha)$ EW corrections were calculated in [7] and full $\mathcal{O}(\alpha)$ EW and $\mathcal{O}(\alpha_s)$ QCD corrections were studied in [8]. In [9], process (1) was considered in the kinematic region where the Higgs boson energy is close to its maximal energy and hence the next-to-leading-logarithmic corrections to the Higgs boson energy distribution can be computed within the nonrelativistic effective theory. Processes of the form $e^+e^- \rightarrow b\bar{b}b\bar{b}W^+W^- \rightarrow b\bar{b}b\bar{b}l^\pm\nu_lq\bar{q}'$ accounting for the signal of associated Higgs boson and top quark pair production, as well as several irreducible background reactions, were studied in [10] and EW contributions to the leptonic and semileptonic reactions (2) have been computed in [11]. Moreover, feasibility of the measurement of the Higgs-top Yukawa coupling at the ILC in reaction (1) was discussed in [12].

Reactions (2), with 8 fermions in the final state, receive contributions typically from a few dozen thousands of the Feynman diagrams already in the lowest order of SM. Most of the diagrams constitute the "non signal" background to the reaction of the associated on shell top quark pair and Higgs boson production and their subsequent decay

$$e^+e^- \rightarrow t\bar{t}H \rightarrow bf_1\bar{f}'_1\bar{b}f_2\bar{f}'_2b\bar{b}, \tag{3}$$

with the same final state as that of (2).

In the present note, we will look into pure off shell effects that are related to the fact that t, $\bar{t}$ and H of (3) are actually produced and they decay as off mass shell particles. To illustrate these effects, we will calculate the cross section of one selected reaction (2) while keeping only the "signal" Feynman diagrams and compare it with the cross in the narrow width approximation (NWA) for the top, antitop and Higgs in the energy range that could be

relevant for the ILC. We will also check whether or not the off shell effects change the prediction of [5] that the cross section of (1) is dominated by the Higgs boson emission off t and $\bar{t}$. We realize that neglecting an overwhelming number of the "non signal" Feynman diagrams may be too crude an approximation, in particular in the energy range not far above the $t\bar{t}H$ threshold. However, our simplified approach has the advantage that it fully takes into account spin correlations that are of great importance in the context of top quark physics [13]. Taking into account the spin correlations would in particular increase the sensitivity to new physics effects, such as an anomalous Wtb couplings [14], especially if the beam polarization is provided at the ILC.

2. Outline of the calculation

We will concentrate on one selected semileptonic channel of reaction (2), namely

$$e^+(p_1)\, e^-(p_2) \;\to\; b(p_3)\, u(p_4)\, \bar{d}(p_5)\, \bar{b}(p_6)\, \mu^-(p_7)\, \bar{\nu}_\mu(p_8)\, b(p_9)\, \bar{b}(p_{10})\,, \quad (4)$$

where the particle four momenta have been indicated in parentheses. In the unitary gauge, reaction (4) receives contributions from 56550 Feynman diagrams already in the lowest order of SM. The corresponding amplitudes can be generated with a Fortran 90 program `carlomat` written by one of the present authors [15]. If we neglect the Higgs boson couplings to fermions lighter than a b-quark then the number of diagrams is reduced to 26816. However, as already stated in Section 1, in order to illustrate the size of the pure off mass shell effect we will restrict ourselves to the lowest order "signal" Feynman diagrams shown in Fig. 2. The corresponding amplitudes are calculated with the helicity amplitude method that had been described in detail in [16] and computed with the use of program libraries described in [17].
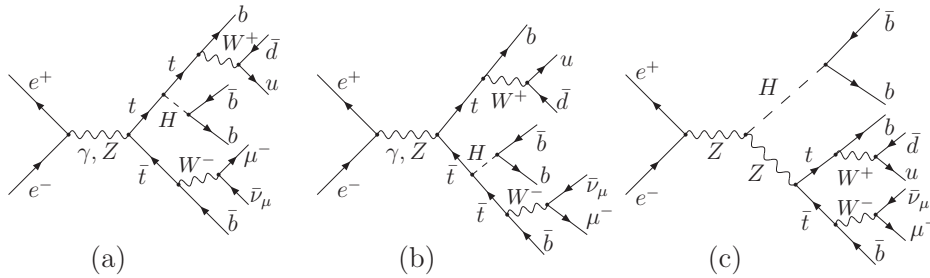

Fig. 2. "Signal" Feynman diagrams of reaction (4).

With that restricted numbers of amplitudes, the actual challenge of the computation of the total cross section of (4) is a right choice of parametrization of the 20-fold phase space integral which should lead to reliable results without using vast numbers of calls to the integrand. The 3 different phase space parametrizations which we use are the following

$$
\begin{aligned}
d^{20}\mathrm{Lips} \;=\; & (2\pi)^{-20} d\mathrm{PS}_2\left(s, s_{345910}, s_{678}\right) d\mathrm{PS}_2\left(s_{345910}, s_{345}, s_{910}\right) \\
& \times\; d\mathrm{PS}_2\left(s_{345}, m_3^2, s_{45}\right) d\mathrm{PS}_2\left(s_{678}, m_6^2, s_{78}\right) \\
& \times\; d\mathrm{PS}_2\left(s_{45}, m_4^2, m_5^2\right) d\mathrm{PS}_2\left(s_{78}, m_7^2, m_8^2\right) d\mathrm{PS}_2\left(s_{910}, m_9^2, m_{10}^2\right) \\
& \times\; ds_{345910} ds_{678} ds_{345} ds_{45} ds_{78} ds_{910}\,,
\end{aligned}
\tag{5}
$$

$$
\begin{aligned}
d^{20}\mathrm{Lips} \;=\; & (2\pi)^{-20} d\mathrm{PS}_2\left(s, s_{345}, s_{678910}\right) d\mathrm{PS}_2\left(s_{345}, m_3^2, s_{45}\right) \\
& \times\; d\mathrm{PS}_2\left(s_{45}, m_4^2, m_5^2\right) d\mathrm{PS}_2\left(s_{678910}, s_{678}, s_{910}\right) \\
& \times\; d\mathrm{PS}_2\left(s_{678}, m_6^2, s_{78}\right) d\mathrm{PS}_2\left(s_{78}, m_7^2, m_8^2\right) d\mathrm{PS}_2\left(s_{910}, m_9^2, m_{10}^2\right) \\
& \times\; ds_{345} ds_{678910} ds_{45} ds_{678} ds_{78} ds_{910}\,,
\end{aligned}
\tag{6}
$$

$$
\begin{aligned}
d^{20}\mathrm{Lips} \;=\; & (2\pi)^{-20} d\mathrm{PS}_2\left(s, s_{345678}, s_{910}\right) d\mathrm{PS}_2\left(s_{345678}, s_{345}, s_{678}\right) \\
& \times\; d\mathrm{PS}_2\left(s_{345}, m_3^2, s_{45}\right) d\mathrm{PS}_2\left(s_{45}, m_4^2, m_5^2\right) d\mathrm{PS}_2\left(s_{678}, m_6^2, s_{78}\right) \\
& \times\; d\mathrm{PS}_2\left(s_{78}, m_7^2, m_8^2\right) d\mathrm{PS}_2\left(s_{910}, m_9^2, m_{10}^2\right) \\
& \times\; ds_{345678} ds_{345} ds_{678} ds_{45} ds_{78} ds_{910}\,.
\end{aligned}
\tag{7}
$$

In Eqs. (5)–(7), $s = (p_1 + p_2)^2$, $s_{ij...} = (p_i + p_j + \ldots)^2$, $i, j = 3, \ldots, 10$, and $d\mathrm{PS}_2\left(q^2, q_1^2, q_2^2\right)$ is a two particle (subsystem) phase space element defined by

$$
d\mathrm{PS}_2\left(q^2, q_1^2, q_2^2\right) = \delta^{(4)}\left(q - q_1 - q_2\right) \frac{d^3 q_1}{2E_1} \frac{d^3 q_2}{2E_2} = \frac{|\vec{q}_1|}{4\sqrt{q^2}} d\Omega_1\,,
\tag{8}
$$

where $\vec{q}_1$ is the momentum and Ω_1 is the solid angle of one of the particles (subsystems) in the relative centre of mass system, $\vec{q}_1 + \vec{q}_2 = 0$.

Parametrizations (5), (6) and (7) have been chosen in such a way that invariants $s_{ij...}$ correspond to virtualities of propagators of the gauge bosons, Higgs boson and/or top quarks in the diagrams of Fig. 2. Possible poles in the propagators of unstable particles are regularized with the constant particle widths Γ_a which are introduced through the complex mass parameters M_a^2 by making the substitution

$$
m_a^2 \;\rightarrow\; M_a^2 = m_a^2 - i m_a \Gamma_a\,, \qquad a = Z, W, H, t\,.
\tag{9}
$$

In order to reduce variance of the MC integration invariants $s_{ij...}$ that are related to the resonating propagators of W, H and t are obtained from the random variables uniformly distributed in the interval $[0, 1]$ by performing mappings smoothing out their Breit–Wigner distributions. Denote the lower

and upper physical limit of $s_{ij\ldots}$ by $s_{ij\ldots}^{\min}$ and $s_{ij\ldots}^{\max}$, respectively, and the uniform random variable by $x \in [0, 1]$, then the mapping is given by

$$s_{ij\ldots} = \Gamma_a m_a \tan\left(\frac{\Gamma_a m_a}{N} x + x_0\right) + m_a^2, \tag{10}$$

with

$$N = \frac{\Gamma_a m_a}{\arctan\left(\frac{s_{ij\ldots}^{\max} - m_a^2}{\Gamma_a m_a} - x_0\right)} \quad \text{and} \quad x_0 = -\arctan\left(\frac{m_a^2 - s_{ij\ldots}^{\min}}{\Gamma_a m_a}\right). \tag{11}$$

Mapping (10) is not performed for s_{345910}, s_{678910} and s_{345678} in the propagators of t in Fig. 2(a), $\bar{t}$ in Fig. 2(b) and Z in Fig. 2(c), respectively, which are far away from resonance in the centre of mass system energy (CMS) range considered. Those three invariants, as well as all the remaining integration variables of Eqs. (5)–(8), which we symbolically denote by $y_j \in [a_j, b_j]$, are obtained from the uniform random variables $x_j \in [0, 1]$ with a simple linear transformation

$$y_j = (b_j - a_j)\, x_j + a_j. \tag{12}$$

Weights w_i, $i = 1, 2, 3$, with which each of the 3 phase space parametrizations (5)–(7) contributes to the total cross section are determined in the initial scanning run performed with all the initial weights equal to $1/3$. They are calculated as the ratios

$$w_i = \frac{\bar{\sigma}_i}{\sum_{j=1}^{3} \bar{\sigma}_j}, \qquad i = 1, 2, 3, \tag{13}$$

where $\bar{\sigma}_i$, $i = 1, 2, 3$, denotes the cross section obtained in the initial scan with phase parametrization (5), (6), (7), respectively. The final result for the total cross section σ of (4) in the "signal" approximation is then calculated as the weighted average

$$\sigma = \sum_{j=1}^{3} w_i \sigma_j \tag{14}$$

with σ_j, $j = 1, 2, 3$ being the cross section computed with phase parametrization (5), (6), (7), respectively.

The cross section of (4) in the NWA, is defined in the following way

$$\sigma_{\text{NWA}} = \sigma(e^+ e^- \to t\bar{t}H) \times \frac{\Gamma_{W^+ \to u\bar{d}}}{\Gamma_W} \times \frac{\Gamma_{W^- \to \mu^- \bar{\nu}_\mu}}{\Gamma_W} \times \frac{\Gamma_{H \to b\bar{b}}}{\Gamma_H}, \tag{15}$$

where $\sigma(e^+ e^- \to t\bar{t}H)$ denotes the total cross section of (1) and we have assumed

$$\frac{\Gamma_{t \to bW^+}}{\Gamma_t} = \frac{\Gamma_{\bar{t} \to \bar{b}W^-}}{\Gamma_t} = 1.$$

The 5-dimensional numerical integration that is necessary in order to compute $\sigma(e^+e^- \to t\bar{t}H)$ does not require the multi-channel MC approach and can be performed with the single phase space parametrization given by

$$d^5\text{Lips} = (2\pi)^{-5}d\text{PS}_2\left(s, s_{t\bar{t}}, m_H^2\right) d\text{PS}_2\left(s_{t\bar{t}}, m_t^2, m_t^2\right) ds_{t\bar{t}}, \qquad (16)$$

where $s_{t\bar{t}} = (p_t + p_{\bar{t}})^2$, with p_t and $p_{\bar{t}}$ being the four momenta of the on shell t and $\bar{t}$ in (1) and the two particle phase space element $d\text{PS}_2$ defined in (8).

The NWA formula of Eq. (15) is obtained from the signal cross section of reaction (4) by making the following substitution for the resonance factors $D_a\left(q^2\right)$, $a = t, W$, corresponding to each of the resonating propagators of the top quark and W-boson in the Feynman diagrams of Fig. 2

$$D_a\left(q^2\right) = \left[\left(q^2 - m_a^2\right)^2 + (m_a\Gamma_a)^2\right]^{-1} \to K_a\delta\left(q^2 - m_a^2\right), \qquad (17)$$

with normalization factors $K_a = \int_{-\infty}^{\infty} dq^2 D_a\left(q^2\right) = \pi/\left(m_a\Gamma_a\right)$. It is just the Dirac delta function on the right hand side of (17) which causes the signal cross section of (4) to take the factorized form of (15). Obviously, substitution (17) makes sense only if the width of unstable particle Γ_a is much smaller than its mass m_a. The relative error associated to it is usually estimated as being of $\mathcal{O}\left(\Gamma_a/m_a\right)$, as required by dimensional analysis. With the values of the top quark and W-boson masses and widths given in Eqs. (19), (20) and (21) we obtain uncertainties of 0.9% and 2.5% for each of the resonating top quark and W-boson propagators. Hence we may expect a discrepancy between the signal and NWA cross sections of the order of a few per cent. This expectations will be confirmed by the actual numerical results which are given in the next section. For a more detailed discussion of limitations of the NWA the reader is referred to [18].

3. Numerical results

The numerical results presented in this section have been obtained with the following set of initial physical parameters. We have chosen the Fermi coupling and fine structure constant in the Thomson limit

$$G_\mu = 1.16639 \times 10^{-5} \text{ GeV}^{-2}, \qquad \alpha_0 = 1/137.03599911, \qquad (18)$$

as well as the W- and Z-boson masses

$$m_W = 80.419 \text{ GeV}, \qquad m_Z = 91.1882 \text{ GeV}, \qquad (19)$$

as the EW input parameters. The top quark mass and the external fermion masses of reaction (4) are the following:

$$m_t = 174.3 \text{ GeV}, \quad m_b = 4.8 \text{ GeV}, \quad m_u = 5 \text{ MeV}, \quad m_d = 10 \text{ MeV}, (20)$$

$$m_e = 0.51099892 \text{ MeV}, \quad m_\mu = 105.6583 \text{ MeV}.$$

The value Higgs boson mass is assumed at $m_H = 130$ GeV. The widths of unstable particles that are introduced through substitution (9) are calculated to the lowest order of SM. This results in

$$\Gamma_t = 1.531 \text{ GeV}, \qquad \Gamma_W = 2.048 \text{ GeV}, \qquad \Gamma_H = 8.065 \text{ MeV}, \qquad (21)$$

for the top quark, W-boson and Higgs boson widths, respectively. The actual value of the Z-boson width is not relevant for our calculation, as the Z-boson propagator is far off its mass shell in all the diagrams of Fig. 2.

The total cross section of reaction (4) calculated with the "signal" diagrams of Fig. 2 is compared with the cross section in the NWA in Table I. We see that the off mass shell effect is of the order of 3% for $\sqrt{s} = 500$–800 GeV, *i.e.* close to the threshold of the associated top quark pair and Higgs boson production, then it decreases and becomes negative, reaching an absolute value of about 5% at $\sqrt{s} = 2$ TeV. This is illustrated in Fig. 3, where both the "signal" and NWA cross sections are plotted as functions of the CMS energy. The off shell effect is caused overwhelmingly by the nonzero widths of the top quarks and W-bosons, as for the assumed value of the Higgs boson mass, $m_H = 130$ GeV, the Higgs boson is very narrow, with a decay width of a few MeV. Actually, the very small lowest order value of 8 MeV for Γ_H in Eq. (21) will be further substantially reduced if the QCD radiative corrections are taken into account, see, *e.g.* [19] and [20].

TABLE I

Total cross sections of reaction (4): the "signal" cross section σ_{signal}, the cross section in NWA σ_{NWA} and their relative difference $\delta = (\sigma_{\text{NWA}} - \sigma_{\text{signal}}) / \sigma_{\text{signal}}$. The numbers in parenthesis show the uncertainty of the last decimals.

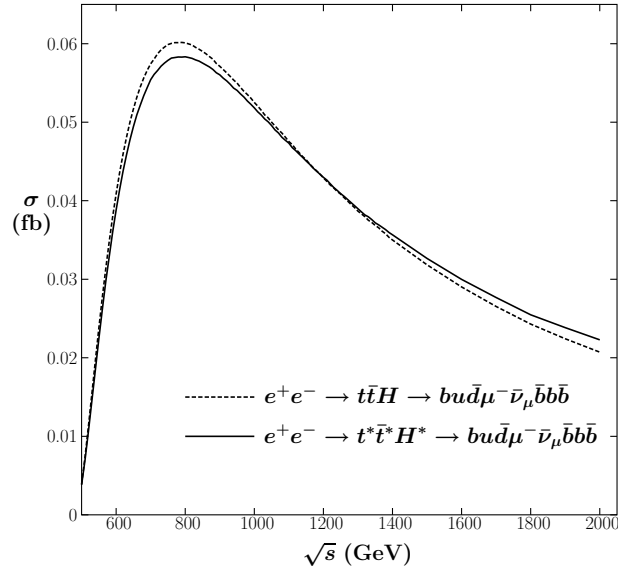| $\sqrt{s}$ [GeV]	σ_{signal} [ab]	σ_{NWA} [ab]	δ [%]
500	3.805(11)	3.923(1)	3.1
800	58.33(7)	60.07(3)	3.0
1000	51.79(7)	52.56(3)	1.5
1200	42.99(6)	42.96(3)	−0.1
2000	21.90(11)	20.76(2)	−5.2

Fig. 3. Total cross sections of reaction (4) as functions of the CMS energy: the "signal" cross section σ_{signal} (solid line) and the cross section in NWA σ_{NWA} (dashed line).

It is interesting to see to which extent the off shell effects may change the prediction of [5] that the cross section of (1) is dominated by the Higgs boson emission off the t- and $\bar{t}$-quark. To this end, in Table II, we present the lowest order "signal" cross section of (4) σ_{signal} and the cross section $\sigma_{\text{signal}}^{\text{no HZZ}}$ that has been calculated with the diagrams of Fig. 2(a) and 2(b), *i.e.* without the Higgsstrahlung off the Z-boson line represented by the diagram of Fig. 2(c). The corresponding results for the cross section in the NWA are given in Table II as σ_{NWA} and $\sigma_{\text{NWA}}^{\text{no HZZ}}$. Let us compare the relative differences shown in Table II as δ_1 and δ_2 defined by

$$\delta_1 = \left(\sigma_{\text{signal}}^{\text{no HZZ}} - \sigma_{\text{signal}}\right)/\sigma_{\text{signal}}, \qquad \delta_2 = \left(\sigma_{\text{NWA}}^{\text{no HZZ}} - \sigma_{\text{NWA}}\right)/\sigma_{\text{NWA}}. \quad (22)$$

They quantify to which extent the Feynman diagram of Fig. 2(c) spoils proportionality of the cross section of (4) to $g_{t\bar{t}H}^2$, which makes the measurement of the top–antitop-Higgs Yukawa coupling more difficult. While δ_1 takes into account the fact that t, $\bar{t}$ and H are produced and decay off mass shell, δ_2 has been calculated assuming that they are on mass shell particles. The lowest order "signal" cross section of (4) σ_{signal} and the "signal" cross section without the diagram of Fig. 2(c) $\sigma_{\text{signal}}^{\text{no HZZ}}$ are plotted as functions of the CMS energy on the left hand side of Fig. 4. The plots on the right hand side of Fig. 4 show the corresponding cross sections in the NWA. Both from Table II and Fig. 4, we see that the Higgsstrahlung off the Z-boson line spoils the

Total cross sections of reaction (4): the "signal" cross section σ_{signal}, the 'signal' cross section calculated without the diagram of Fig. 2(c) $\sigma_{\text{signal}}^{\text{no ZZH}}$, the cross section in the NWA σ_{NWA}, the cross section in the NWA calculated without the diagram of Fig. 2(c) $\sigma_{\text{NWA}}^{\text{no ZZH}}$ and the relative differences δ_1 and δ_2 of (22). The numbers in parenthesis show the uncertainty of the last decimals.

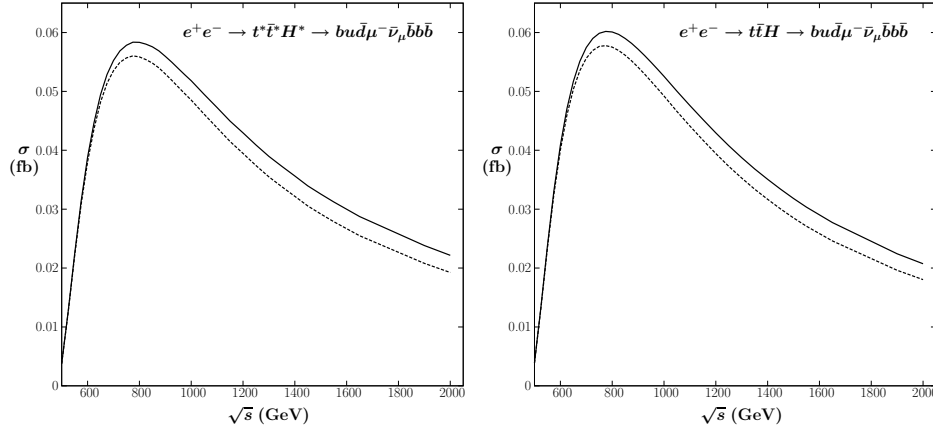| $\sqrt{s}$ [GeV]	σ_{signal} [ab]	$\sigma_{\text{signal}}^{\text{no HZZ}}$ [ab]	δ_1 [%]	σ_{NWA} [ab]	$\sigma_{\text{NWA}}^{\text{no HZZ}}$ [ab]	δ_2 [%]
500	3.805(11)	3.775(10)	-0.8	3.923(1)	3.886(1)	-0.9
800	58.33(7)	55.84(6)	-4.3	60.07(3)	57.51(3)	-4.3
1000	51.79(7)	48.52(6)	-6.3	52.56(3)	49.23(3)	-6.3
1200	42.99(6)	39.50(7)	-8.1	42.96(3)	39.41(3)	-8.3
2000	21.90(11)	19.18(12)	-12.4	20.76(2)	18.03(2)	-13.2

Fig. 4. The lowest order cross sections of (4) as functions of the CMS energy. On the left hand side: the "signal" cross section (solid line) and the "signal" cross section without the diagram of Fig. 2(c) (dashed line); on the right hand side: the corresponding cross sections in the NWA.

proportionality of the total cross section of the associated $t\bar{t}H$ production to $g_{t\bar{t}H}^2$ almost in the same way, independently of whether the off shell effects are taken into account or not.

4. Summary and outlook

We have looked at a role that the off shell effects may play in reaction (1) of the associated production of the top quark pair and Higgs boson at the ILC. We have illustrated these effects for a semileptonic reaction (4), which is one of the detection channels of (1) at the ILC, by comparing the "signal" cross section that has been calculated by performing 20-fold integration of the squared matrix element while keeping only the "signal" Feynman diagrams with the cross section in the NWA. The off shell effects are typically of the order of a few per cent for the CMS energies in the range from 500 GeV to 2 TeV, in accordance with the expectation based on the discussion of the quality of the NWA in the end of Section 2. We have also shown that the off shell effects do not affect much the prediction of [5] that the cross section of (1) is dominated by the Higgs boson emission off t and $\bar{t}$, which makes it an attractive tool for determination of the Higgs–top Yukawa coupling.

The presented approach is very simplified, as a lot of the "non signal" background Feynman diagrams have been neglected in the calculation of the lowest order cross section of (4), but it has the advantage that it fully takes into account spin correlations that are of great importance in the context of top quark physics. Further work is needed in order to take into account a complete set of the lowest Feynman diagrams and include leading radiative corrections for reactions (2).

REFERENCES

[1] J.A. Aguilar-Saavedra *et al.* [ECFA/DESY LC Physics Working Group Collaboration], `hep-ph/0106315`; T. Abe *et al.*, [American Linear Collider Working Group Collaboration], `hep-ex/0106056`; K. Abe *et al.* [ACFA Linear Collider Working Group Collaboration], `hep-ph/0109166`.

[2] Ch. Parkes, International Conference on High Energy Physics, `http://lephiggs.web.cern.ch/LEPEWWG`, July 2006.

[3] R. Barate *et al.*, *Phys. Lett.* **B565** (2003) 61.

[4] B. Kilminster, `hep-ex/0611001`, to appear in the proceedings of 33rd International Conference on High Energy Physics (ICHEP 06), Moscow, Russia, 26 July–2 August, 2006.

[5] A. Djouadi, J. Kalinowski, P.M. Zerwas, *Mod. Phys. Lett.* **A7**, 1765 (1992); A. Djouadi, J. Kalinowski, P.M. Zerwas, *Z. Phys.* **C54**, 255 (1992).

[6] S. Dittmaier, M. Kramer, Y. Liao, M. Spira, P.M. Zerwas, *Phys. Lett.* **B441**, 383 (1998); S. Dittmaier, M. Kramer, Y. Liao, M. Spira, P.M. Zerwas, *Phys. Lett.* **B478**, 247 (2000); S. Dawson, L. Reina, *Phys. Rev.* **D57**, 5851 (1998); S. Dawson, L. Reina, *Phys. Rev.* **D59**, 054012 (1999).

[7] Yu You *et al.*, *Phys. Lett.* **B571**, 85 (2003);
A. Denner, S. Dittmaier, M. Roth, M.M. Weber, *Phys. Lett.* **B575**, 290 (2003).

[8] G. Bélanger *et al.*, *Phys. Lett.* **B571**, 163 (2003).

[9] C. Farrel, A.H. Hoang, *Phys. Rev.* **D72**, 014007 (2005).

[10] S. Moretti, *Phys. Lett.* **B452**, 338 (1999).

[11] C. Schwinn, `hep-ph/0412028`.

[12] H. Baer, S. Dawson, L. Reina, *Phys. Rev.* **D61**, 013002 (2000); A. Juste, G. Merino, `hep-ph/9910301`; A. Juste, ECONF C0508141:ALCPG0426, 2005, `hep-ph/0512246`; A. Gay, *Eur. Phys. J.* **C49**, 489 (2007) [`hep-ph/0604034`].

[13] M. Jeżabek, J.H. Kühn, *Nucl. Phys.* **B320**, 20 (1989).

[14] B. Grządkowski, Z. Hioki, *Phys. Lett.* **B476**, 87 (2000); *Phys. Lett.* **B529**, 82 (2002); *Phys. Lett.* **B557**, 55 (2003); S.D. Rindani, *Pramana* **54**, 791 (2000), [`hep-ph/0002006`]; K. Kołodziej, *Phys. Lett.* **B584**, 89 (2004).

[15] K. Kołodziej, "`carlomat`, a program for generation of lowest order amplitudes", in preparation.

[16] K. Kołodziej, M. Zrałek, *Phys. Rev.* **D43**, 3619 (1991); F. Jegerlehner, K. Kołodziej, *Eur. Phys. J.* **C12**, 77 (2000).

[17] K. Kołodziej, *Comput. Phys. Commun.* **151**, 339 (2003); K. Kołodziej, F. Jegerlehner, *Comput. Phys. Commun.* **159**, 106 (2004).

[18] N. Kauer, `hep-ph/0703077`.

[19] A. Djouadi, J. Kalinowski, M. Spira, *Comput. Phys. Commun.* **108**, 56 (1998).

[20] F. Jegerlehner, K. Kołodziej, T. Westwański, *Eur. Phys. J.* **C44**, 195 (2005).